Mathematical Biosciences and Engineering

http://www.aimspress.com/journal/MBE

MBE, 23(3): 547–566.
DOI: 10.3934/mbe.2026021
Received: 17 November 2025
Revised: 07 January 2026
Accepted: 08 January 2026
Published: 27 January 2026

Research article

Modular arithmetic as an alternative to model seasonal time-varying transmission rates: Influenza as a case study

Woldegebriel Assefa Woldegerima* **and Nickson Golooba**

Disease-informed Modelling, Methods & Systems (DIMMS) Lab, Department of Mathematics & Statistics, Faculty of Science, York University, Toronto, ON, Canada

* **Correspondence:** Email: wassefaw@yorku.ca.

Abstract: Seasonal infectious diseases like influenza pose a recurrent challenge to public health. While compartmental models, such as the susceptible-infectious-recovered-susceptible (SIRS) framework, are standard tools, representing the time-varying transmission rate, $\beta(t)$, in an interpretable yet effective manner remains a key challenge. Existing established alternative methods for modeling seasonality use sinusoidal forcing functions, flexible splines, etc. In this paper, we propose and apply a modular approach where $\beta(t)$ is defined using distinct, epidemiologically intuitive seasonal rates, with smooth transitions between them. To begin, we develop this framework as a theoretical tool, demonstrating its capacity to generate realistic, recurring seasonal outbreaks under plausible parameter assumptions. We then calibrate and assess this model against real-world, monthly laboratory-confirmed influenza surveillance data from Ontario, Canada, for the pre-pandemic period of 2014–2019. A systematic optimization using a coarse grid search followed by stochastic refinement calibrates the model to the observed data. The calibrated model, featuring a mean immunity duration of approximately 235 days, achieves a strong fit with the historical case data (Pearson correlation $r = 0.80$). Our results demonstrate that this modular arithmetic-based framework is a practical and effective tool for modeling real-world influenza dynamics, successfully bridging the gap between theory and empirical surveillance.

Keywords: modular arithmetic; seasonality; influenza; SIRS model; parameter estimation; model calibration

1. Introduction

We all know that illnesses like the common cold and influenza (the flu) tend to show up more often during certain times of the year. For many places, that means flu season hits hard in the fall and winter and then seems to almost disappear in the summer. This regular pattern, happening year after year, is what we call "seasonality" [1]. Understanding why this happens and being able to predict these peaks is

really important for hospitals, doctors, and public health officials. It helps them prepare for busy times, decide when to run vaccination campaigns, and give timely advice to the public.

Influenza is a perfect example of a seasonal disease. It causes millions of illnesses worldwide each year, leading to hospitalizations and, unfortunately, deaths [2]. Because it comes back reliably each year, but its intensity can vary, having good models to predict its spread is crucial.

For decades, scientists have used mathematical models to understand how diseases spread. A common starting point is the susceptible-infectious-recovered (SIR) or susceptible-infectious-recovered-susceptible (SIRS) model [3, 4]. These models divide the population into groups: susceptible (people who can get sick), infectious (people who are sick and spreading it), and recovered (people who are immune, at least for a while). The 'S' at the end of SIR**S** means that recovered individuals can eventually become susceptible again. This process of waning immunity is critical for modeling recurrent diseases like influenza, as the constant return of individuals to the susceptible state is what allows for repeated seasonal outbreaks rather than a single epidemic that confers lasting immunity [5].

While these models are useful basic tools, they often have a big limitation: they usually assume the disease spreads at the same rate all year long. They use a constant number, often called β (beta), to represent how easily the disease jumps from an infected person to a susceptible one. But for the flu, we know this is not true. Something about winter makes it spread more easily than summer, maybe it is the weather, maybe it is because we spend more time indoors, or maybe kids are back in school [6, 7]. Whatever the exact reasons (and it is likely a mix), the transmission rate β definitely changes with the seasons. Ignoring this makes simple SIR/SIRS models unable to predict those yearly peaks and troughs.

1.1. How researchers usually handle seasonality

Scientists know about this problem, of course, and have tried different ways to add seasonality into their models, including the following:

Smooth waves (sine functions): A standard approach is to use a sine wave to let β oscillate over the year [6, 8]. While mathematically simple, these models assume that transmission changes slowly, which often fails to capture the sharp shifts seen when schools reopen [9].

Contact structure and behavior: Other models focus on human behavior by using age-structured contact matrices. These can simulate how transmission slows during school holidays and increases during term time [10]. These are biologically detailed but require extensive data on mixing patterns that are not always available. More advanced approaches determine expected changes in contact patterns using kinetic models and optimal control theory, offering rigorous methods for defining transmission policies [11–13].

Complex functions or data: Some models link transmission directly to climate variables, such as absolute humidity [14, 15]. A popular and intuitive way to explain influenza's seasonality is by linking it to the weather. Many models make the transmission rate, $\beta(t)$, a direct function of temperature or humidity, based on strong evidence that the virus survives and spreads more effectively in cold and dry air [7, 14, 16]. While this approach is biologically appealing, it faces several practical challenges that can limit its use.

These models require detailed weather data that is not always available or complete for every location, which complicates their application on a global scale [17]. Furthermore, the specific relationship between climate and influenza can vary dramatically by latitude; a model built for a temperate city, for instance,

may not work in a tropical one [7]. This complexity can also make the models themselves difficult to interpret. When several weather factors are included, it can be hard to identify which ones are truly driving transmission, a challenge highlighted by recent model analyses [18]. Finally, a model based on weather cannot account for sudden changes in human behavior, such as school holidays, which are known to significantly reduce contact rates and slow an outbreak [9].

1.2. Our approach: Using modular arithmetic for clear seasons

We therefore sought a modeling approach for seasonality that was both epidemiologically interpretable and straightforward to implement within standard compartmental frameworks. Our idea was to use **modular arithmetic**, the math of remainders, like telling time on a clock. We treat the year as a cycle (say, $m = 365$ days). By looking at the day number within the year using the modulo operator ($t \pmod m$), we can instantly know which part of the cycle we are in.

We then define the transmission rate β as a piecewise function based on this underlying principle:

- If $t \pmod m$ falls within the "winter" range, use β_{winter}.
- If $t \pmod m$ falls within the "spring" range, use β_{spring}.
- And so on for summer and fall.

This creates a transmission rate that changes in steps, staying constant within each defined season but changing clearly between them. While sharp steps might not be perfectly realistic (so we smooth the transitions slightly in our final implementation for better numerical behavior and realism), the underlying principle is that modular arithmetic provides a clear, structured way to tell the model "it is winter now, spread rate is high" or "it is summer now, spread rate is low". This seems less common in the literature than smooth sine waves, especially as the primary defining mechanism for seasonality. We believe this approach is highly interpretable and the β values directly correspond to the average transmission potential during epidemiologically relevant periods.

Our analysis first establishes the theoretical capacity of the modular SIRS framework to generate seasonal dynamics and respond to interventions. We then calibrate the model's key parameters, the seasonal transmission rates, and the duration of waning immunity, by fitting the model to monthly influenza surveillance data from Ontario (2014–2019).

The predictable seasonality of influenza and the role of waning immunity make it an ideal test case for this modeling approach. In this paper, we do the following:

1) Describe the SIRS model incorporating a seasonal transmission rate, $\beta(t)$, defined by modular arithmetic principles, and demonstrate its theoretical capacity to generate realistic, recurring outbreak patterns.
2) Calibrate the model's key parameters, specifically the seasonal transmission rates and the duration of waning immunity, by fitting the model to public health surveillance data from Ontario for the years 2014–2019.
3) Evaluate the performance of the calibrated model by quantifying its goodness-of-fit to the observed historical data.
4) Use the theoretical framework and the insights from the calibrated model to analyze the impact of factors like immunity duration and to explore the potential effectiveness of seasonally-timed public health interventions.

By doing this, we aim to demonstrate that modular arithmetic offers a valuable, clear, and effective tool for modeling seasonal infectious diseases like influenza. The rest of this paper details our methods, presents the simulation results, and discusses their implications.

2. Methods

This section describes the mathematical model, the specific implementation of seasonal transmission using modular arithmetic principles, the parameters chosen to represent influenza dynamics, and the numerical methods used for simulation.

2.1. The SIRS model structure

We adapt the SIRS compartmental model. This framework is appropriate for diseases like influenza, where individuals recover, but immunity is not permanent and can wane over time. The population is divided into three compartments:

- $S(t)$: The proportion of the population susceptible to infection at time t.
- $I(t)$: The proportion of the population currently infectious at time t.
- $R(t)$: The proportion of the population recovered and temporarily immune at time t.

The total population proportion is constant, $S(t) + I(t) + R(t) = 1$. The dynamics of these compartments over time are described by the following system of ordinary differential equations (ODEs):

$$\frac{dS}{dt} = -\beta(t)SI + \omega R \tag{2.1}$$

$$\frac{dI}{dt} = \beta(t)SI - \gamma I \tag{2.2}$$

$$\frac{dR}{dt} = \gamma I - \omega R \tag{2.3}$$

Here:

- $\beta(t)$ is our model's time-varying transmission rate (units: day^{-1}), which changes throughout the year to capture seasonal effects. We build this function by first assigning a distinct base rate to each of the four seasons. The final, continuous $\beta(t)$ is then generated using a Gaussian-weighted smoothing method that blends these base rates, as detailed in Section 2.2.
- γ is the recovery rate. The average duration of infectiousness is $1/\gamma$.
- ω is the rate at which recovered individuals lose their immunity and return to the susceptible compartment. The average duration of immunity is $1/\omega$.

The inclusion of the waning immunity term, ωR is what fundamentally characterizes this framework as a model for a seasonally endemic disease, as opposed to a self-limiting epidemic. In theoretical epidemiology, endemic persistence requires a continuous replenishment of the susceptible population. In our model, the ωR term fulfills this role. This serves a similar function to the demographic processes of birth (Λ) and death ($d_1 S$) found in the classic epidemic models, which also ensure the susceptible pool does not become permanently depleted. Preventing the disease from 'burning out', this mechanism makes it possible for seasonal changes in the transmission rate, $\beta(t)$, to drive the recurrent annual epidemics we observe with influenza.

2.2. Defining seasonal transmission $\beta(t)$ using modular arithmetic principles

To formalize the seasonal forcing, we first introduce a piecewise constant function, $\beta_{\text{base}}(t)$, which represents the unsmoothed seasonal transmission rate. Let $m = 365$ days be the length of the epidemiological year and $L = m/4 \approx 91.25$ days be the length of one season. The base transmission rate is given by:

$$\beta_{\text{base}}(t) = \begin{cases} \beta_{\text{spring}}, & 0 \le d < L, \\ \beta_{\text{summer}}, & L \le d < 2L, \\ \beta_{\text{fall}}, & 2L \le d < 3L, \\ \beta_{\text{winter}}, & 3L \le d < m, \end{cases}$$

where $d = t \bmod m$ (with $t = 0$ corresponding to day 1), and the coefficients on the right-hand side are the constant transmission rates for each season.

To ensure that $\beta(t)$ is continuous and avoid unrealistic jumps, we implement a smoothing method. For the theoretical analysis, we utilized linear interpolation over a 10-day transition window. For the data-driven Ontario calibration, we utilized Gaussian kernel smoothing on a monthly scale. Specifically, for any month $m \in \{1, \ldots, 12\}$, $\beta(t)$ is calculated as the weighted sum of the four seasonal base rates β_s:

$$\beta(t) = \frac{\sum_s \beta_s \cdot \exp\left(-\frac{\text{dist}(m,\mu_s)^2}{2\sigma^2}\right)}{\sum_s \exp\left(-\frac{\text{dist}(m,\mu_s)^2}{2\sigma^2}\right)}, \tag{2.4}$$

where μ_s is the center month of each season (e.g., January for winter), and $\text{dist}(m, \mu_s)$ is the circular distance on a 12-month cycle. In the calibration, we set $\sigma = 0.8$ months to ensure that the model captures the distinct transmission potential of each season while maintaining continuity at the boundaries, as established in kernel smoothing theory [19].

While the modular arithmetic defines the base seasonal rates, instantaneous jumps in $\beta_{\text{base}}(t)$ at seasonal boundaries are epidemiologically unrealistic and can introduce numerical stiffness into the differential equations. To create a smooth, continuous transmission rate $\beta(t)$, we implemented a blending method based on Gaussian weights. This technique is a form of nonparametric kernel smoothing, a well-established statistical method for creating smooth functions from discrete data points, which we have adapted for the circular nature of the annual cycle [19]. The explicit mathematical definition of this smoothing is provided in Eq (2.4). For any given day, the final transmission rate, $\beta(t)$, is calculated as a weighted average of the four base seasonal rates. The weights are determined by the proximity of that day to the center of each season on a 365-day circular calendar, with the width of the Gaussian smoothing controlled by a tunable parameter, σ_{months}. This approach, analogous in principle to other flexible methods like splines used in modern epidemiology [20, 21], ensures that $\beta(t)$ varies smoothly while preserving the distinct average transmission levels characteristic of each season (Figure 1).

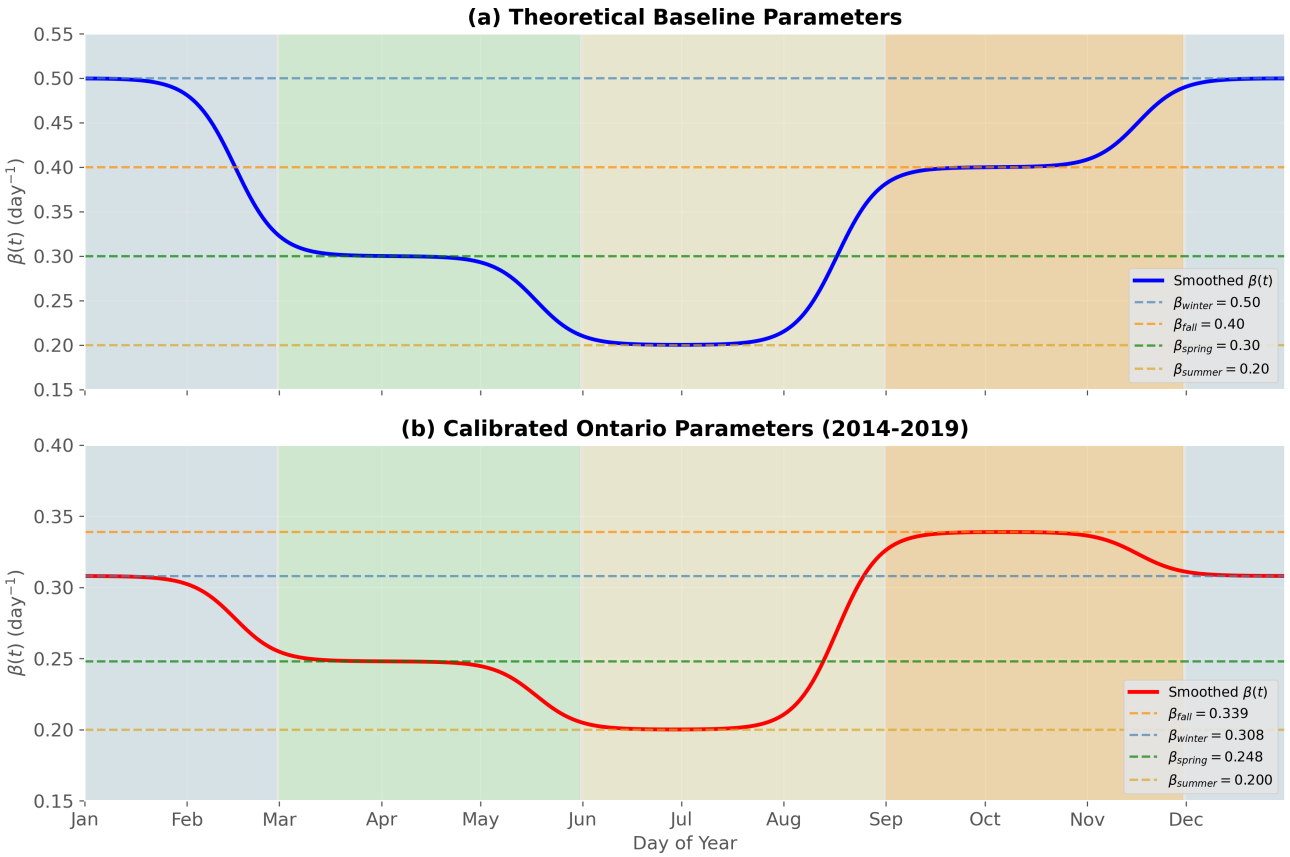

Figure 1. The smoothed seasonal transmission rate $\beta(t)$ over a 365-day cycle. (a) Theoretical baseline parameters with seasonal R_0 values ranging from 1.0 (summer) to 2.5 (winter). (b) Calibrated parameters from fitting to Ontario surveillance data (2014–2019), showing a higher fall transmission ($\beta_{\text{fall}} = 0.339$) than winter ($\beta_{\text{winter}} = 0.308$). Shaded regions indicate meteorological seasons. Dashed horizontal lines show the underlying seasonal base rates. The smooth transitions are achieved using Gaussian-weighted blending with $\sigma = 0.8$ months.

For simplicity, our model partitions the year into four equal seasons of about 91 days each. We recognize that astronomical seasons are not perfectly equal in length, but this approximation is a common and practical choice in quarterly SIRS models, having a negligible impact on the year-scale dynamics we are interested in [15, 22]. It is also worth noting that our framework is flexible; Season lengths, L, could easily be replaced with calendar-aligned values to achieve finer detail without changing the underlying smoothing method.

2.3. Theoretical model parameters

For the initial theoretical simulations, parameters were chosen to reflect established epidemiological characteristics of seasonal influenza in a temperate climate.

Baseline transmission and recovery. We take the mean infectious period to be $1/\gamma = 5$ days, so $\gamma = 0.20$ day^{-1}, following [23]. Those same guidelines, together with large multi-country reviews, place

the basic reproduction number in the range of $R_0 \approx 1.3$–2.0 [24]. Our chosen parameters align with these estimates.

Our chosen parameters, resulting in a seasonal R_0 range of 1.0 to 2.5, were selected to create a clear and strong seasonal signal for the purpose of exploring the model's theoretical behavior and its response to interventions.

- **Seasonal modulation of β.** Models based on absolute humidity levels reproduce U.S. mortality curves only when $\beta(t)$ varies by 40–90% between winter and summer [15]. Guided by that, we therefore set our seasonal values as:

$$\beta_{\text{winter}} = 0.50,\ \beta_{\text{fall}} = 0.40,\ \beta_{\text{spring}} = 0.30,\ \beta_{\text{summer}} = 0.20\ \text{day}^{-1}.$$

  This represents a 60% swing that keeps R_0 between ≈ 2.5 in winter and ≈ 1.0 in summer. These values seed the model with realistic seasonal dynamics capable of driving pronounced winter outbreaks.
- **Waning immunity rate (ω):** We primarily used $\omega = 1/365\ \text{day}^{-1}$, corresponding to an average duration of immunity of one year (365 days) for the baseline scenario. We also explored the impact of varying this duration (90, 180, and 730 days, and permanent immunity where $\omega = 0$) in specific analyses.
- **Cycle length (m):** $m = 365$ days.
- **Smoothing of $\beta(t)$ transitions:** The transitions between seasonal β values were smoothed using the Gaussian-weighted method described in Section 2.2, with a characteristic smoothing width of $\sigma_{\text{months}} = 0.8$ months.

These parameters result in seasonal R_0 values of approximately 2.50 (winter), 2.00 (fall), 1.50 (spring), and 1.00 (summer), which fluctuate around the epidemic threshold ($R_0 = 1$), driving the seasonal outbreaks observed.

2.4. Numerical simulation

The system of ODEs (Eqs (2.1)–(2.3)) was solved numerically using Python. For the theoretical explorations and scenario analyses, we used the high-level adaptive step-size Runge-Kutta (RK45) integrator provided by the `scipy.integrate.solve_ivp` function, with outputs evaluated at daily intervals. For the computationally intensive model calibration process, a more efficient daily-step explicit Euler integration scheme was implemented. In both cases, daily incidence was calculated and then aggregated to monthly totals for analysis and plotting. To ensure that the rapid seasonal transitions did not introduce numerical instability, we cross-validated our results using implicit solvers suitable for stiff equations (backward differentiation formula and Radau methods); the resulting dynamics were identical, confirming that the sharp oscillations in R_{eff} are structural features of the seasonal forcing rather than integration artifacts.

Initial conditions for the theoretical simulations were set to $S(0) = 0.999$, $I(0) = 0.001$, and $R(0) = 0.0$. For the data calibration, the initial infectious fraction, I_0, was treated as a free parameter to be estimated, with $S(0) = 1 - I_0$ and $R(0) = 0$.

2.5. Analysis metrics and intervention modeling

In addition to tracking the proportions $S(t), I(t), R(t)$, we calculated several key metrics to evaluate the disease dynamics and the impact of public health measures:

- **Daily new cases:** As a primary measure of disease incidence, we tracked the rate of new infections occurring each day, calculated as $\beta(t)S(t)I(t)$.
- **Effective reproduction number ($R_{\mathbf{eff}}(t)$):** This represents the average number of secondary infections caused by a single infectious individual at time t, given the current susceptible population and transmission rate. It was calculated as:

$$R_{\text{eff}}(t) = \frac{\beta(t)S(t)}{\gamma}$$

  An $R_{\text{eff}}(t) > 1$ indicates that the system is above the epidemic threshold, favoring growth, while $R_{\text{eff}}(t) < 1$ indicates that infections will recede. The oscillation of $R_{\text{eff}}(t)$ driven by our seasonal $\beta(t)$ is the direct mechanism for the recurrent outbreaks in our model.
- **Intervention modeling:** To evaluate the potential impact of seasonally targeted strategies, we modeled five scenarios by reducing the transmission rate β starting from the second year of simulation. The intervention transmission rate is defined as $\beta_{\text{intervention}} = \beta_{\text{season}} \times (1 - r)$, where r is the reduction factor. The strategies included the following:
  - **No Intervention:** The baseline scenario ($r = 0$).
  - **Winter-Only:** A 30% reduction applied only to β_{winter}.
  - **Fall-Winter:** A 30% reduction applied to both β_{fall} and β_{winter}.
  - **All-Season (Weighted):** A risk-proportional strategy with reductions of 10% in spring, 10% in summer, 30% in fall, and 40% in winter.
  - **Intensive Winter:** An aggressive 50% reduction applied specifically to β_{winter}.

For each scenario, the total disease burden was quantified by summing the daily new infections within each season over the simulation period, allowing for a direct comparison of how the timing of interventions alters the cumulative case count.

2.6. Model calibration against surveillance data

In order to assess the performance of our theoretical model in reality, we performed a calibration process using real-world surveillance data, as implemented in our data-fitting notebook.

Data source and simulation span. We obtained monthly laboratory-confirmed influenza case counts for Ontario, Canada, for the pre-pandemic period of January 2014 to December 2019. The model was simulated over this exact window to generate monthly case totals for comparison. For figures, the final fitted trajectory was extended for visualization purposes, but these forecast months were excluded from the fitting process.

Optimization process. We conducted a systematic, two-stage optimization to find the parameters that best fit the observed data. The parameters estimated were the four seasonal transmission rates, collectively denoted as β_{season}, the waning immunity rate (ω), and the initial proportion of infectious individuals (I_0). The process was as follows:

1) **Coarse grid search:** To begin, we conducted a broad search over a pre-defined grid of plausible values for all six key parameters.
2) **Stochastic local search:** The best parameter set from the grid search was then used as the starting point for a fine-tuning process. This involved a stochastic local search with a decaying step size, where small, normally distributed perturbations were made to the parameters over 180 iterations. A new parameter set was accepted only if it resulted in a lower objective function value, allowing the model to converge on a precise local optimum. The proposal step size was annealed by a factor of 0.985 at each iteration to focus the search as it approached the optimum.

The grid for the coarse search spanned plausible ranges for each parameter, including three to four values for each season; β for example, $\beta_{\text{winter}} \in \{0.32, 0.38, 0.44\}$, three values for the mean immunity duration (180, 240, and 365 days) and four values for I_0 (2×10^{-5} to 1×10^{-3}). The stochastic refinement consisted of 180 iterations with a normally distributed proposal step, where the step size was normalized by a factor of 0.985 at each iteration. All simulations were seeded for reproducibility.

Objective function and scaling. We measured the goodness-of-fit using a winter-weighted RMSE. To prioritize accuracy during the months of highest clinical burden, we assigned a weight $w_k = 1.25$ to winter observations (December through February) and $w_k = 1.0$ for the remainder of the year. The objective function J is defined as:

$$J = \sqrt{\frac{1}{N}\sum_{k=1}^{N} w_k (C_{\text{obs},k} - \kappa C_{\text{sim},k})^2} + \lambda P(\theta), \tag{2.5}$$

where $C_{\text{obs},k}$ is the observed case count, $C_{\text{sim},k}$ is the simulated monthly incidence, and κ is a scale factor re-estimated via least squares. To guide the optimization toward an epidemiologically sensible hierarchy ($\beta_{\text{winter}} \geq \beta_{\text{fall}} \geq \beta_{\text{spring}} \geq \beta_{\text{summer}}$), we included a soft monotonicity penalty $P(\theta)$ with a weight of $\lambda = 200$. This penalty is calculated as the sum of squared differences for any seasonal rates that violate this hierarchical order. The final performance is reported via RMSE and the Pearson correlation r.

During the calibration process, the Gaussian parameters, specifically the smoothing width ($\sigma = 0.8$ months) and the seasonal midpoints (μ_s) were held constant. The centers were fixed to align with the meteorological peaks of each season (January, April, July, and October). We treated σ as a fixed hyperparameter to ensure the structural identifiability of the seasonal transmission rates. By fixing the transition width, we prevent the optimization from confounding the duration of a season with its intensity, allowing for a unique and stable estimation of the average transmission potential (β) for each quarter.

3. Results

Our analysis is presented in two parts. To begin, we detail the results from the theoretical SIRS model, demonstrating its capability to generate and explore seasonal disease dynamics under various assumptions. We then present the results from the calibration of this model against historical influenza data from Ontario, thereby demonstrating its practical applicability.

3.1. Theoretical model dynamics and scenario analysis

The theoretical SIRS model, defined by the modular arithmetic framework with smoothed transitions, was simulated to establish its baseline behavior and sensitivity. Parameters were chosen to reflect plausible influenza dynamics, including seasonal basic reproduction numbers (R_0) ranging from 1.00 in summer to 2.50 in winter, and a baseline average immunity duration of 365 days (see Section 2).

Baseline seasonal pattern generation. The model successfully generated recurrent, seasonal outbreaks consistent with influenza patterns. As illustrated in Figure 2, the system settles into a repeating pattern of distinct seasonal outbreaks following an initial large epidemic. The proportion of infected individuals (I, top panel) peaks during the winter months, while the effective reproduction number ($R_{\text{eff}}(t)$, bottom panel) oscillates across the epidemic threshold ($R = 1$), driving the seasonal rise and fall of infections.

The concentration of disease burden in the fall and winter months is clearly visible in the incidence peaks and the elevated effective reproduction number shown in Figure 2. Throughout the simulated years, $R_{\text{eff}}(t)$ remains consistently above the epidemic threshold during these high-transmission periods, confirming the model's capacity to produce a robust and predictable seasonal signal without the need for additional data-driven forcing.

Impact of immunity duration and intervention strategies. The theoretical framework was then employed to explore key epidemiological scenarios. An analysis of varying immunity durations (Figure 3) demonstrates that shorter immunity periods for example, 90 and 180 days result in larger and more regular annual outbreaks. This is because the susceptible pool replenishes more rapidly, providing the necessary fuel for subsequent epidemics and highlighting the critical role of waning immunity in sustaining seasonal disease patterns.

Furthermore, we simulated several seasonally-targeted intervention strategies to evaluate their potential impact. The results, summarized in Figure 4, show how interventions alter the total disease burden within each season over the 4-year simulation. For the "No Intervention" scenario, Winter is the dominant contributor to the total case load. Interventions that specifically target high-transmission seasons, such as the "Intensive Winter (50% reduction)" strategy, effectively reduce this seasonal burden. The "All-Season (Weighted)" strategy demonstrates the largest overall reduction by lowering case counts across all seasons, highlighting its epidemiological effectiveness.

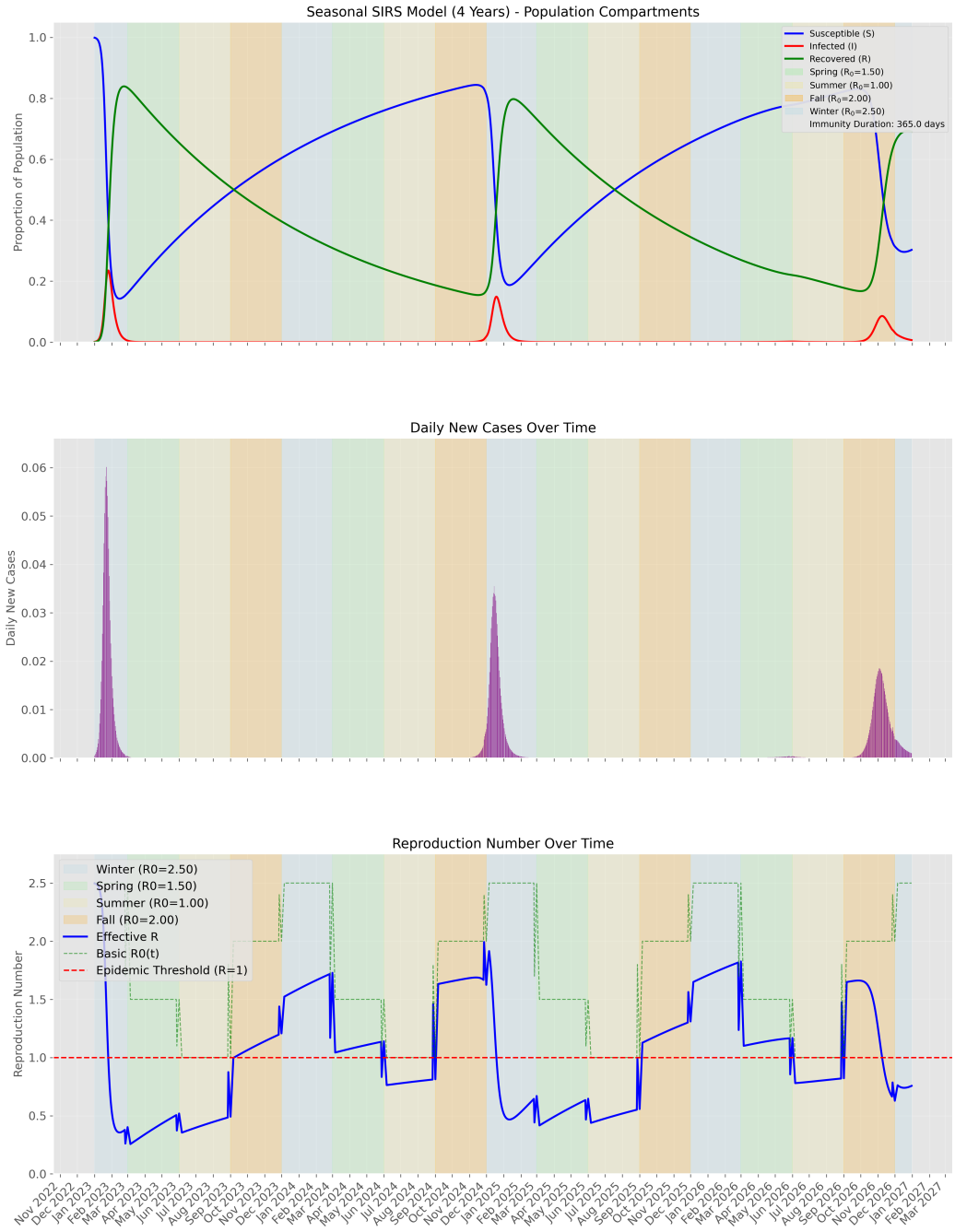

Figure 2. Baseline seasonal SIRS model dynamics simulated over a four-year period using theoretical parameters. (Top) Temporal evolution of the population compartments: susceptible (S, blue), infected (I, red), and recovered (R, green). (Middle) Daily incidence of new cases over time. (Bottom) Comparison of the effective reproduction number ($R_{\text{eff}}(t)$, blue solid line) against the seasonal basic reproduction number ($R_0(t)$, green dashed line) and the epidemic threshold ($R = 1$, red dashed line). The sharp transitions in R_{eff} reflect the rapid seasonal shifts defined by the modular transmission function and are not numerical artifacts. Shaded background regions indicate the meteorological seasons, with corresponding R_0 values ranging from 1.0 (summer) up to 2.5 (winter).

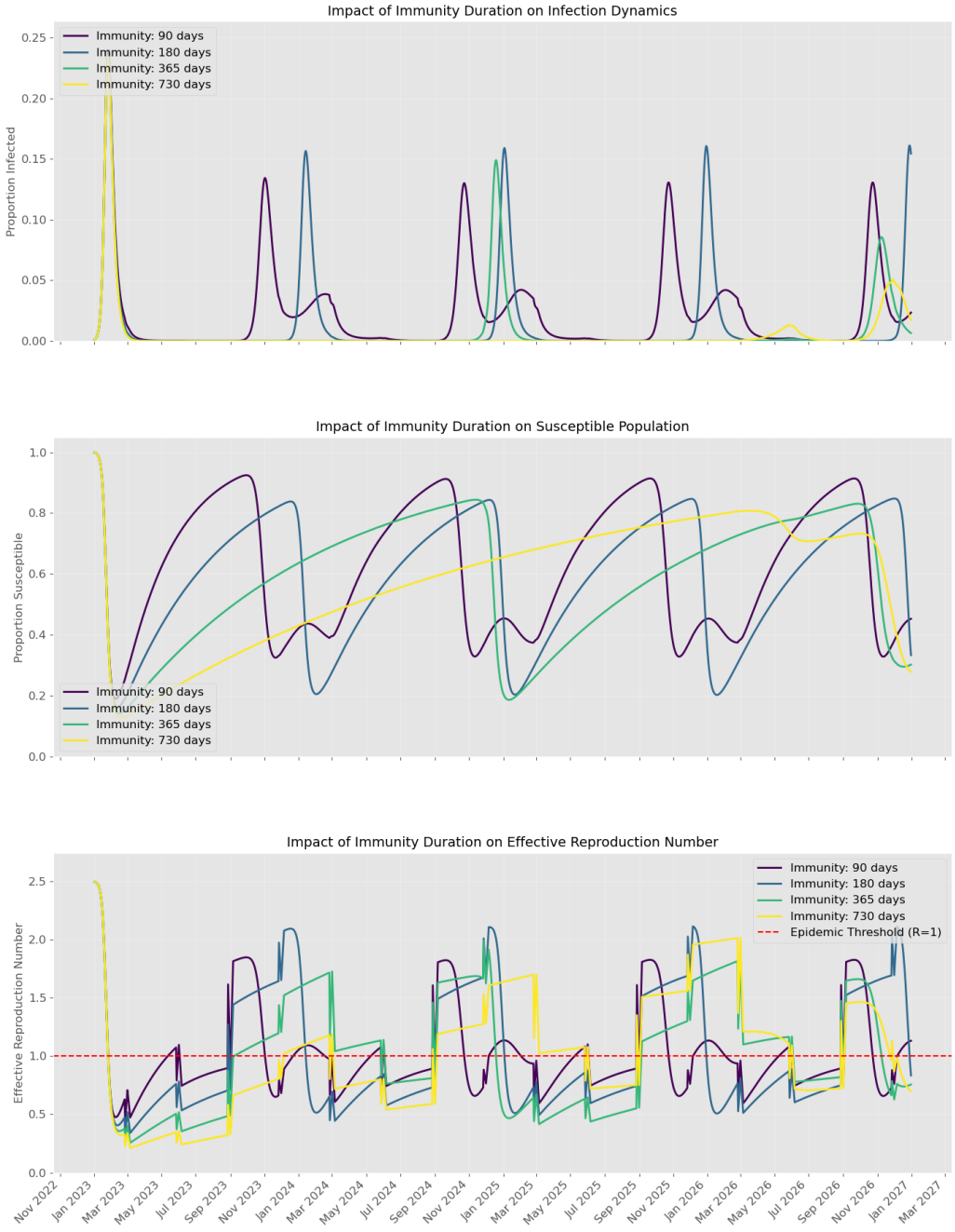

Figure 3. Impact of different immunity durations on key model outputs over 4 years in the theoretical model, showing: (Top) proportion infected, (Middle) proportion susceptible, and (Bottom) effective reproduction number (R_{eff}). Note: The rapid oscillations correspond to the seasonal boundaries defined in the modular framework.

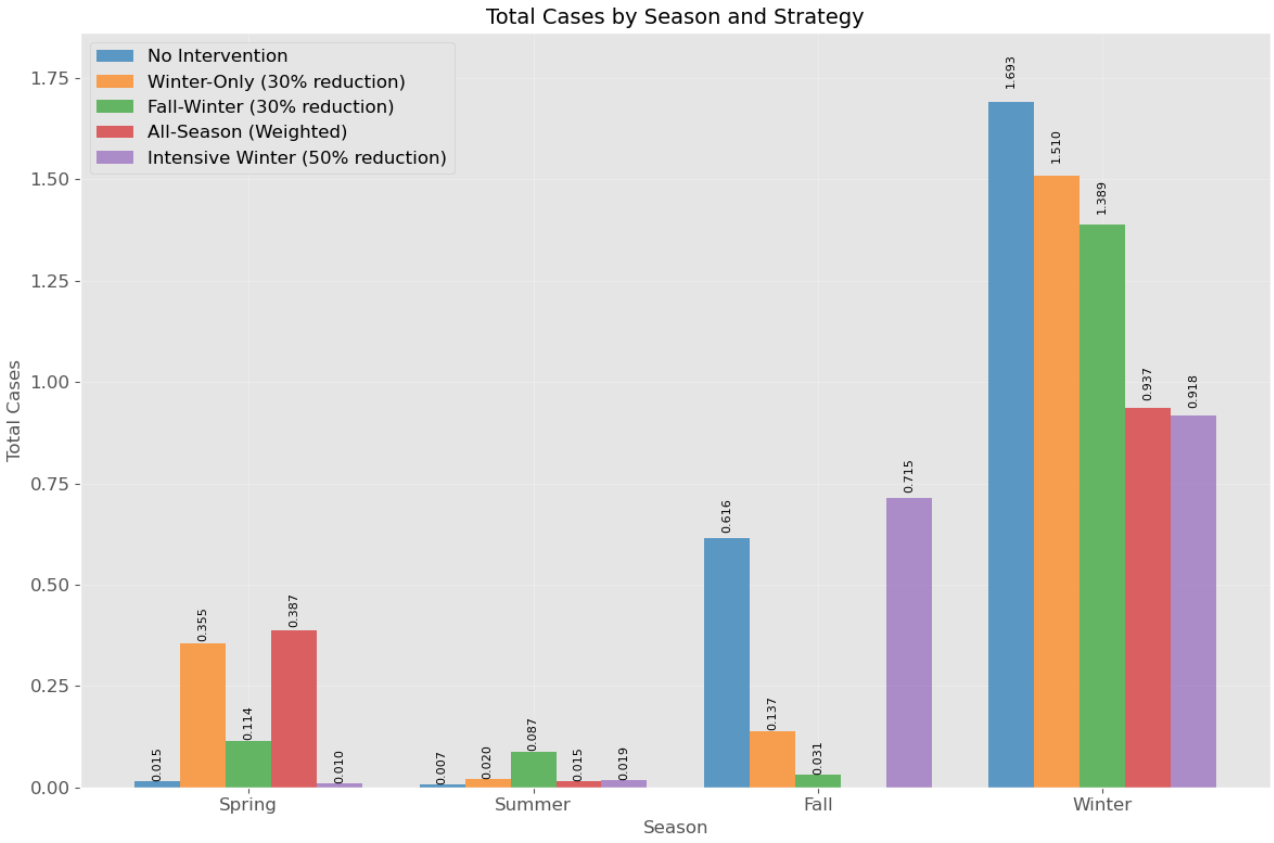

Figure 4. Total new cases aggregated by season and strategy over a 4-year simulation period. The height of each bar represents the total cumulative cases occurring within that season under a specific intervention strategy.

3.2. Model calibration with Ontario data

After establishing the model's theoretical soundness, we calibrated it against monthly laboratory-confirmed influenza case data from Ontario for the pre-pandemic period of 2014–2019. The two-stage optimization process (see Section 2.6) identified a single set of parameters that best fit the observed surveillance data.

The optimization revealed that the model best matched the historical data with a mean immunity duration of 234.7 days (approximately 7.8 months). This empirically derived value is crucial, as it is shorter than the one-year period often assumed and was necessary to accurately capture the inter-annual dynamics in the Ontario data. The final calibrated transmission rates (β) were determined to be:

$$\beta_{\text{winter}} = 0.308 \text{ day}^{-1}, \beta_{\text{fall}} = 0.339 \text{ day}^{-1}, \beta_{\text{spring}} = 0.248 \text{ day}^{-1}, \textit{and } \beta_{\text{summer}} = 0.200 \text{ day}^{-1}.$$

These values correspond to seasonal R_0 numbers of approximately 1.54, 1.69, 1.24, and 1.00, respectively, providing a data-driven picture of influenza's seasonality in this region.

The performance of the final, calibrated model is presented in Figure 5. The model's simulated monthly cases (blue line) show a strong correspondence with the observed counts (orange dots),

achieving a Pearson correlation of $r = 0.80$. The framework successfully captures the timing and relative magnitude of the seasonal peaks, demonstrating its effectiveness in replicating real-world influenza patterns when calibrated with surveillance data.

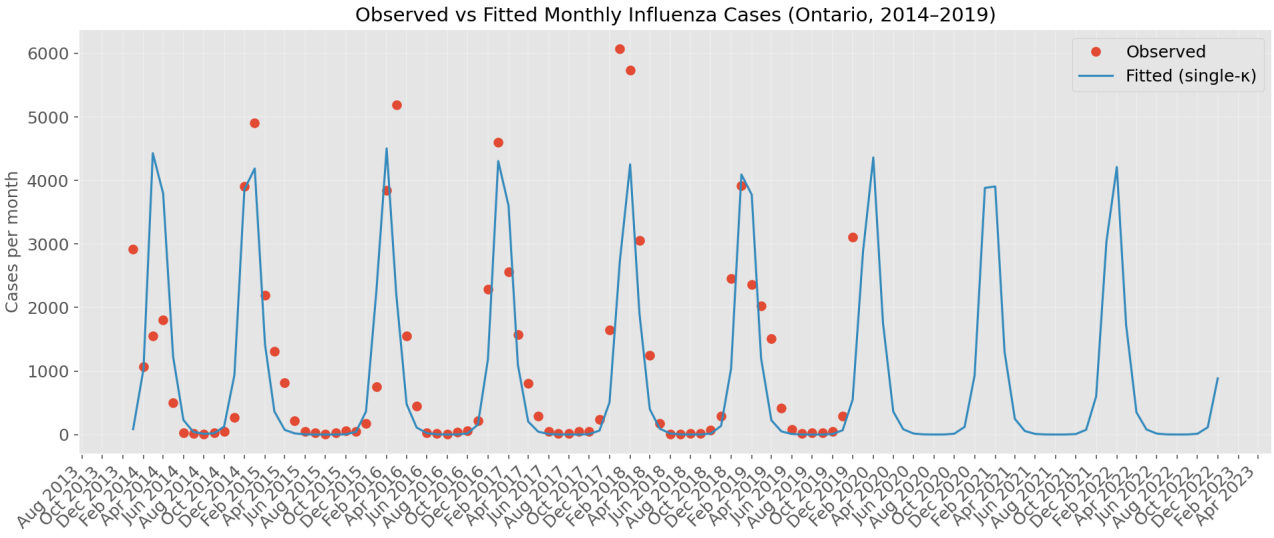

Figure 5. Observed vs. Fitted monthly influenza cases for Ontario, 2014–2019. Orange dots represent the actual surveillance data from Public Health Ontario. The blue line shows the output of the calibrated SIRS model. The model's fitted curve is extended for three years post-observation to illustrate the projected dynamics under the calibrated parameters.

4. Discussion

In this study, we developed, analyzed, and calibrated an SIRS model that uses a modular arithmetic framework to represent seasonal variations in disease transmission. Our primary objective was to create a model that is both epidemiologically interpretable and capable of reproducing the recurrent outbreaks characteristic of influenza. By first establishing the model's theoretical capabilities and then grounding it with real-world surveillance data, we have demonstrated the utility of this approach.

4.1. Model performance: From theoretical patterns to empirical fit

The initial theoretical simulations successfully demonstrated that our modular framework is a sound basis for modeling seasonal diseases. By defining distinct base transmission rates for each season (β_{season}) and smoothing the transitions, the model generated the expected dynamics: clear infection peaks during high-transmission seasons (fall/winter) and troughs during low-transmission periods (summer), as shown in Figure 2. While the resulting oscillations in the effective reproduction number (R_{eff}) are more abrupt than those produced by sinusoidal forcing, this accurately reflects our "modular" hypothesis: that transmission operates in distinct regimes driven by sharp behavioral or environmental shifts, rather than continuous, gentle variation.

The calibration against Ontario influenza data (Figure 5) assesses the model's goodness-of-fit against empirical observations. We believe that achieving a Pearson correlation of $r = 0.80$ with observed

cases from 2014–2019 demonstrates that a structured, piecewise definition of seasonality can effectively replicate the complex patterns found in empirical data. Note that we utilize the Pearson correlation here as a descriptive metric of trend alignment rather than for formal hypothesis testing, given the auto-correlated nature of time-series data. This provides a compelling alternative to more abstract methods like sinusoidal forcing functions, as our seasonal β values can be more directly interpreted as the average transmission potential during distinct, epidemiologically relevant periods of the year.

An interesting and non-intuitive result from the calibration was the ordering of the fitted transmission rates, with fall ($\beta_{\text{fall}} = 0.339$) having a slightly higher rate than winter ($\beta_{\text{winter}} = 0.308$). This finding, which emerged despite a soft prior encouraging a monotonic decrease from winter to summer, suggests a nuanced dynamic. While winter may have conditions most favorable for viral survival, the effective spread in the fall could be amplified by behavioral factors, such as the return to school and increased indoor mixing after the summer. Furthermore, the model's dynamics are state-dependent; the large number of new infections during the fall depletes the susceptible pool, meaning that even with a high potential transmission rate in winter, the number of available susceptibles ($S(t)$) is lower, thus moderating the overall force of infection. This highlights the model's ability to capture complex interactions between seasonal forcing and population-level immunity.

Comparison with alternative forcing methods. Our modular approach offers a distinct alternative to established methods like sinusoidal forcing, where $\beta(t)$ oscillates symmetrically [8]. While sinusoidal models are mathematically elegant, they often struggle to capture the sharp shifts in transmission linked to school terms or sudden behavioral changes [9]. Climate-driven models, which use variables like absolute humidity, provide strong mechanistic insights [7, 15] but require high-resolution meteorological data that is not always available. More flexible statistical methods, such as periodic splines, can achieve high accuracy but often sacrifice interpretability for fit [20]. Our framework occupies a middle ground: it provides the interpretability of seasonal regimes without requiring external climate data, allowing public health officials to discuss 'average winter transmission' in a way that maps directly to calendar-based planning.

The role of model simplicity and demographics. It is important to note that our SIRS framework is a closed-population model, meaning it does not include demographic processes such as births and deaths. This was a deliberate choice to isolate and test the effectiveness of our novel modular seasonality mechanism in its simplest form. However, the real-world Ontario data to which we calibrated the model is from an open population where demographics, particularly the continuous influx of new susceptibles via births, undoubtedly play a role in long-term disease dynamics.

We believe this simplification is a key reason for the nature of our calibrated fit. While the model with its 235-day immunity period successfully captures the primary seasonal oscillations and inter-annual variability, the absence of demographics likely contributes to some of the remaining discrepancies between the fitted curve and the observed data points. The replenishment of the susceptible pool in our model is driven solely by waning immunity (ωR), whereas in reality, it is a combination of waning immunity and new births. For future work, incorporating demographic terms into the model is a logical next step. While this would add complexity, it would likely improve the model's ability to capture the finer details of long-term endemic persistence and could potentially yield an even more precise fit to the surveillance data.

4.2. The critical role of waning immunity: An empirical estimate

Our theoretical analysis of varying immunity durations (Figure 3) reinforces a fundamental principle of endemic dynamics: replenishing the susceptible pool through waning immunity is essential for enabling recurrent annual outbreaks. Shorter immunity periods led to more regular and pronounced annual epidemics in our simulations, as the population's overall susceptibility recovered more quickly.

Crucially, the data calibration process provided a specific, data-driven estimate for this parameter. The optimization routine converged on a mean immunity duration of approximately 235 days. This finding is consistent with immunological studies suggesting that influenza protection can wane significantly within a single year [25]. Our estimate also aligns with the theoretical work of Dushoff et al. [5], who demonstrated that the interaction between rapid immunity loss and seasonal forcing is the primary driver of annual periodicity. Furthermore, as noted by Ranjeva et al. [26], this rapid replenishment of the susceptible pool is essential for explaining the recurrent peaks seen in longitudinal surveillance data.

This finding is significant for two reasons. First, it is shorter than the one-year duration often used as a baseline in theoretical models, suggesting that the rate of immunity loss may be faster than commonly assumed, at least in the context of capturing aggregate population dynamics. Second, this shorter duration was essential for the model to accurately reproduce the observed inter-annual variability in the Ontario data without producing overly large, biennial outbreaks. This result highlights that the interaction between the period of immunity loss and the annual cycle of seasonal forcing is a key determinant of real-world influenza patterns, and our model provides a framework for estimating this interaction from surveillance data.

4.3. Implications for public health interventions

The theoretical model also served as a valuable tool for exploring the potential impact of seasonally-targeted public health interventions. As summarized in Figure 4, the analysis of total cases by season provides clear, quantitative insights for public health planning. The bar chart unequivocally shows that, under baseline conditions, winter is the primary driver of the annual disease burden. Consequently, interventions that reduce transmission during the high-risk fall and winter seasons have the most significant impact. For instance, the "intensive winter (50% reduction)" strategy demonstrates a marked decrease in the winter case load. This reinforces the importance of timing interventions, such as vaccination campaigns and public health messaging, to coincide with these periods of highest risk. Furthermore, the model allows for a direct comparison of strategies, showing that while a targeted winter intervention is effective, a broader "all-season (weighted)" approach can yield an even greater overall reduction in cases by mitigating transmission throughout the entire year.

Limitations and future directions: Although the model successfully integrates the theoretical structure with empirical data, several limitations should be acknowledged. The model assumes homogeneous mixing and does not include the age structure. Our seasonal β values are phenomenological; they capture the effect of seasonality without explicitly modeling the underlying drivers. Additionally, the model is deterministic and does not account for stochastic events that can influence outbreaks. Crucially, the current framework lacks a probabilistic formulation to explicitly account for the uncertainty inherent in aggregated surveillance data; incorporating such stochasticity, for example, via stochastic differential equations, is a necessary next step. We also do not explicitly

model the effects of viral evolution (antigenic drift) as a separate mechanism, but instead our waning immunity parameter ω phenomenologically captures the combined effect of intrinsic immune loss and viral drift, a simplification consistent with other mathematical frameworks describing recurrent epidemics [27, 28].

These limitations define several promising avenues for future research. True external validation would require testing the calibrated model on an independent dataset, for example, data from a different time period or region, which represents a critical next step to establish the generalizability of the modular approach. Applying this calibration framework to data from other geographical regions would also test the robustness of the modular approach.

5. Conclusions

In this paper, we proposed and calibrated a seasonal SIRS model for influenza dynamics based on the principle of modular arithmetic. Our primary contribution is the demonstration of a two-stage workflow where this interpretable theoretical framework was developed and then successfully calibrated against real-world public health surveillance data.

Our theoretical simulations confirmed that a modular definition of the transmission rate, $\beta(t)$, is sufficient to generate the recurrent, seasonal outbreaks characteristic of influenza. This framework also proved to be a flexible tool for exploring the impact of key epidemiological parameters, such as immunity duration, and for comparing the potential effectiveness of various seasonally-timed intervention strategies.

Crucially, when applied to historical influenza case data from Ontario (2014–2019), the model achieved a strong empirical fit (Pearson correlation $r = 0.80$). The calibration process yielded a data-driven estimate of approximately 235 days for the average duration of immunity, a key parameter that significantly influenced the model's ability to replicate observed inter-annual dynamics. This successful calibration elevates the model from a purely theoretical construct to a practical tool with demonstrated relevance to real-world disease patterns.

While acknowledging the limitations inherent in compartmental models, our work establishes that a modular arithmetic approach to seasonality offers a valuable, clear, and effective alternative to more abstract functional forms. It provides a robust and interpretable framework for modeling seasonal infectious diseases, successfully bridging the gap between epidemiological theory and empirical public health data. This method holds promise for future applications in forecasting, scenario analysis, and the ongoing effort to better predict and control seasonal epidemics.

Code and data availability

The public surveillance data used for this study was obtained from Public Health Ontario. The full Python code used to generate all simulations, figures, and results presented in this paper is available upon email request from the corresponding author.

Use of AI tools declaration

No generative AI tools were used in the preparation of this manuscript.

Funding statement

This research is funded by the NSERC Discovery Grant (Appl. No.: RGPIN-2023-05100). Both authors also equally acknowledge the financial support from the Canadian Institute for Health Research (CIHR) under the Mpox and other zoonotic threats Team Grant (FRN. 187246). W.A.W also thanks the article publishing harge fee (APC) support received from York University Small Research Grant.

Conflict of interest

All authors declare no conflicts of interest in this paper.

References

1. S. Altizer, A. Dobson, P. Hosseini, P. Hudson, M. Pascual, P. Rohani, Seasonality and the dynamics of infectious diseases, *Ecol. Lett.*, **9** (2006), 467–484. https://doi.org/10.1111/j.1461-0248.2005.00879.x
2. A. D. Iuliano, K. M. Roguski, H. H. Chang, D. J. Muscatello, R. Palekar, S. Tempia, et al., Estimates of global seasonal influenza-associated respiratory mortality: A modelling study, *The Lancet*, **391** (2018), 1285–1300. https://doi.org/10.1016/S0140-6736(17)33293-2
3. W. O. Kermack, A. G. McKendrick, A contribution to the mathematical theory of epidemics, *Proc. R. Soc. London A*, **115** (1927), 700–721. https://doi.org/10.1098/rspa.1927.0118
4. H. W. Hethcote, The mathematics of infectious diseases, *SIAM Rev.*, **42** (2000), 599–653. https://doi.org/10.1137/S0036144500371907
5. J. Dushoff, J. B. Plotkin, S. A. Levin, D. J. Earn, Dynamical resonance can account for seasonality of influenza epidemics, *Proc. Natl. Acad. Sci. U.S.A.*, **101** (2004), 16915–16916. https://doi.org/10.1073/pnas.0407293101
6. E. Lofgren, N. H. Fefferman, Y. N. Naumov, J. Gorski, E. N. Naumova, Influenza seasonality: Underlying causes and modeling theories, *J. Virol.*, **81** (2007), 5429–5436. https://doi.org/10.1128/JVI.01680-06
7. J. D. Tamerius, J. Shaman, W. J. Alonso, K. Bloom-Feshbach, C. K. Uejio, A. Comrie, et al., Environmental predictors of seasonal influenza epidemics across temperate and tropical climates, *PLoS Pathog.*, **9** (2013), e1003194. https://doi.org/10.1371/journal.ppat.1003194
8. M. J. Keeling, P. Rohani, *Modeling Infectious Diseases in Humans and Animals*, Princeton University Press, 2008. https://doi.org/10.1515/9781400841035
9. S. Cauchemez, A. J. Valleron, P. Y. Boelle, A. Flahault, N. M. Ferguson, Estimating the impact of school closure on influenza transmission from sentinel data, *Nature*, **452** (2008), 750–754. https://doi.org/10.1038/nature06732
10. J. Mossong, N. Hens, M. Jit, P. Beutels, K. Auranen, R. Mikolajczyk, et al., Social contacts and mixing patterns relevant to the spread of infectious diseases, *PLoS Med.*, **5** (2008), e74. https://doi.org/10.1371/journal.pmed.0050074

11. G. Dimarco, B. Perthame, G. Toscani, M. Zanella, Kinetic models for epidemic dynamics with social heterogeneity, *J. Math. Biol.*, **83** (2021), 4. https://doi.org/10.1007/s00285-021-01630-1
12. G. Dimarco, G. Toscani, M. Zanella, Optimal control of epidemic spreading in the presence of social heterogeneity, *Philos. Trans. R. Soc. A*, **380** (2022), 20210160. https://doi.org/10.1098/rsta.2021.0160
13. A. Bondesan, G. Toscani, M. Zanella, Kinetic compartmental models driven by opinion dynamics: Vaccine hesitancy and social influence, *Math. Models Methods Appl. Sci.*, **34** (2024), 1043–1076. https://doi.org/10.1142/S0218202524400062
14. J. Shaman, M. Kohn, Absolute humidity modulates influenza survival, transmission, and seasonality, *Proc. Natl. Acad. Sci. U.S.A.*, **106** (2009), 3243–3248. https://doi.org/10.1073/pnas.0806852106
15. J. Shaman, V. E. Pitzer, C. Viboud, B. T. Grenfell, M. Lipsitch, Absolute humidity and the seasonal onset of influenza in the continental united states, *PLoS Biol.*, **8** (2010), e1000316. https://doi.org/10.1371/journal.pbio.1000316
16. A. C. Lowen, S. Mubareka, J. Steel, P. Palese, Influenza virus transmission is dependent on relative humidity and temperature, *PLoS Pathog.*, **3** (2007), e151. https://doi.org/10.1371/journal.ppat.0030151
17. M. New, D. Lister, M. Hulme, I. Makin, A high-resolution data set of surface climate over global land areas, *Clim. Res.*, **21** (2002), 1–25. https://doi.org/10.3354/cr021001
18. C. Zhang, X. Zhang, Y. Bai, E. H. Lau, S. Pei, The structural identifiability of a humidity-driven epidemiological model of influenza transmission, *Viruses*, **14** (2022), 2795. https://doi.org/10.3390/v14122795
19. M. P. Wand, M. C. Jones, *Kernel Smoothing*, CRC Press, 1994. https://doi.org/10.1201/b14876
20. S. N. Wood, *Generalized Additive Models: An Introduction with R*, Chapman and Hall/CRC, 2017. https://doi.org/10.1201/9781315370279
21. A. G. Kummer, J. Zhang, C. Jiang, M. Litvinova, P. C. Ventura, M. A. Garcia, et al., Evaluating seasonal variations in human contact patterns and their impact on the transmission of respiratory infectious diseases, *Influenza Other Respir. Viruses*, **18** (2024), e13301. https://doi.org/10.1111/irv.13301
22. N. M. Ferguson, D. A. Cummings, C. Fraser, J. C. Cajka, P. C. Cooley, D. S. Burke, Strategies for mitigating an influenza pandemic, *Nature*, **442** (2006), 448–452. https://doi.org/10.1038/nature04795
23. World Health Organization, *Pandemic Influenza Preparedness and Response: A WHO Guidance Document*, 2009. Available from: https://www.ncbi.nlm.nih.gov/books/NBK143060/.
24. M. Biggerstaff, S. Cauchemez, C. Reed, M. Gambhir, L. Finelli, Estimates of the reproduction number for seasonal, pandemic, and zoonotic influenza: A systematic review of the literature, *BMC Infect. Dis.*, **14** (2014), 480. https://doi.org/10.1186/1471-2334-14-480
25. S. Cobey, S. E. Hensley, Immune history and influenza virus susceptibility, *Curr. Opin. Virol.*, **22** (2017), 105–111. https://doi.org/10.1016/j.coviro.2016.12.004

26. S. Ranjeva, R. Subramanian, V. J. Fang, G. M. Leung, D. K. Ip, R. A. Perera, et al., Age-specific differences in the dynamics of protective immunity to influenza, *Nat. Commun.*, **10** (2019), 1660. https://doi.org/10.1038/s41467-019-09652-6

27. J. B. Plotkin, J. Dushoff, S. A. Levin, Hemagglutinin sequence clusters and the antigenic evolution of influenza a virus, *Proc. Natl. Acad. Sci. U.S.A.*, **99** (2002), 6263–6268. https://doi.org/10.1073/pnas.082110799

28. S. A. Levin, J. Dushoff, J. B. Plotkin, Evolution and persistence of influenza a and other diseases, *Math. Biosci.*, **188** (2004), 17–28. https://doi.org/10.1016/j.mbs.2003.08.010

AIMS Press